

## New levels in $^{168}\text{Er}$ : Use of a Compton-suppressed Ge array with the $(n, \gamma)$ reaction

R. L. Gill,<sup>1</sup> R. F. Casten,<sup>1,2</sup> W. R. Phillips,<sup>3</sup> B. J. Varley,<sup>3</sup> C. J. Lister,<sup>4</sup> J. L. Durell,<sup>3</sup> J. A. Shannon,<sup>3</sup>  
and D. D. Warner<sup>5</sup>

<sup>1</sup>*Department of Physics, Brookhaven National Laboratory, Upton, New York 11973-5000*

<sup>2</sup>*Wright Nuclear Structure Laboratory, Yale University, New Haven, Connecticut 06520-8124*

<sup>3</sup>*Department of Physics and Astronomy, University of Manchester, Manchester, M13 9PL, United Kingdom*

<sup>4</sup>*Department of Physics, Argonne National Laboratory, Argonne, Illinois 60439*

<sup>5</sup>*Daresbury Laboratory, Warrington, WA4 4AD, United Kingdom*

(Received 15 May 1996)

For the first time an  $(n, \gamma)$  reaction has been extensively studied using a large array of Compton-suppressed Ge detectors (the TESSA array). The nucleus  $^{168}\text{Er}$  was studied and the data show substantial improvement, in both quantity and quality, over previous coincidence data. Even though  $^{168}\text{Er}$  is perhaps the best studied deformed nucleus, over 250 new coincidence relations and a number of new levels in  $^{168}\text{Er}$  were disclosed, demonstrating the usefulness of this approach. Nuclear physics applications relate to the extension of nearly complete spectroscopy to higher excitation energies and to the study of statistical and chaotic features of the decay of low spin compound nuclear levels. [S0556-2813(96)03011-7]

PACS number(s): 23.20.Lv, 25.40.Lw, 27.70.+q

### I. INTRODUCTION

Large Compton-suppressed arrays of high-resolution high-purity Ge detectors are a crucial tool in modern experimental nuclear physics. Many recent discoveries, especially in the fields of high-spin phenomena and spectroscopy far from stability, would have been extremely difficult, if not impossible, to achieve without the use of such devices. However, in spite of the well-known power of these arrays, none, to the knowledge of these authors, has ever been used at a reactor facility to study levels populated in neutron capture reactions. It would be interesting to do so, however, since the  $(n, \gamma)$  reaction produces a large number of coincident  $\gamma$  rays, but yet accesses an entirely different spin range of levels than heavy-ion reactions. The cascade of transitions following neutron capture feeds levels with population falling off with the difference between target ground state spin and final level spin. Typically, states with about  $4\hbar$  above the target spin are populated significantly. The TESSA array was therefore taken to Brookhaven National Laboratory (BNL) to perform experiments at the High Flux Beam Reactor (HFBR). This array [1], originally constructed at the Daresbury Laboratory, employs 16 Ge detectors with bismuth germanate (BGO) Compton suppression shields. Separate measurements of  $\gamma$ - $\gamma$  coincidences following thermal neutron fission of  $^{235}\text{U}$ , and following thermal neutron capture of  $^{167}\text{Er}$ , were performed. The fission measurements studied prompt fission  $\gamma$  rays. The  $^{167}\text{Er}$  measurements examined excited levels in  $^{168}\text{Er}$  that are populated by prompt  $\gamma$  emission after neutron capture. Since the ground state of  $^{168}\text{Er}$  is  $\frac{7}{2}^-$ , final states with spins from 0 to about 7 should be observed. It is the purpose of this paper to present and discuss the results of the  $^{167}\text{Er}(n, \gamma)^{168}\text{Er}$  reaction.

In 1981, Davidson *et al.* [2] published the results of a comprehensive study of excited states in  $^{168}\text{Er}$  that are populated by the  $(n, \gamma)$  reaction. The resulting level scheme was based on extensive data from the GAMS (Gamma Spectrom-

eter) facility at the ILL (Institut Laue Langevin), and ARC (Average Resonance Capture) measurements at BNL, and provided a fertile testing ground for many nuclear models, especially the IBA (interacting boson approximation). Later, Davidson and Dixon [3] attempted to extend the level scheme with additional data, and by searching for additional energy sums that could give rise to states beyond the pairing gap. The work of Ref. [3] became the basis for an update to the Nuclear Data Sheets evaluation for the  $^{168}\text{Er}$  level scheme [4,5]. Still more recently, Jungclaus *et al.* [6] collected a substantial number of  $\gamma$ - $\gamma$  coincidences (also at the BNL HFBR) taken with three, non-Compton-suppressed, Ge detectors in an experiment which was sensitive to  $\gamma$  intensities as low as 3 per 10 000 neutron captures. The data of Jungclaus *et al.* showed that without either the ultra high-precision  $\gamma$ -ray energy measurements possible with GAMS, or the use of  $\gamma$ - $\gamma$  coincidences, assignments based solely on energy sums must be viewed with skepticism. This is especially true for nuclei (such as  $^{168}\text{Er}$ ) with a large number of excited states, which can lead to many accidental energy sums.

The results of the measurements of Jungclaus *et al.*, which led to the proposal of 19 new levels, suggested that a modern  $\gamma$ -ray detector array, such as TESSA, may provide even higher sensitivity. At the outset, this issue is not clear since multiplicities are relatively low (typically three to four  $\gamma$ -ray steps for the neutron capture state to the ground state) and, since Doppler effects are negligible, a small set of detectors can be placed closer to the target than is possible with a large array. The extensive existing data and the complexity of its  $\gamma$ -ray spectrum make  $^{168}\text{Er}$  an ideal testing ground for investigating the value of such an array for the study of neutron capture reactions. The sensitivity of the array can be readily assessed by determining the lower limit for observing coincidences with low-intensity  $\gamma$  rays since most of the observed  $\gamma$  rays from neutron capture on  $^{167}\text{Er}$  are already placed in the level scheme.

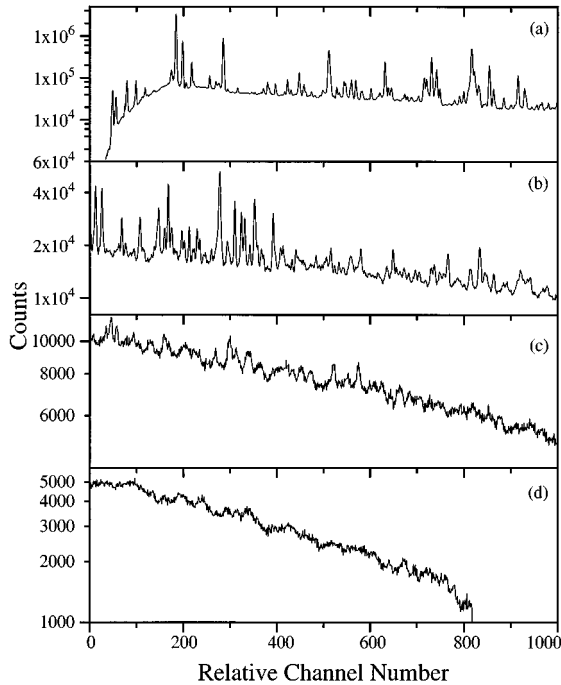


FIG. 1. The projection of all twofold  $\gamma$ - $\gamma$  coincidences is shown on semilogarithmic plots. The large number and density of  $\gamma$  rays in this spectrum illustrate the difficulties that were encountered in setting some gates. (a) shows the range from channels 0–1000, (b) shows channels 1000–2000, (c) shows channels 2000–3000, and (d) shows channels 3000–4000. One channel corresponds to approximately 1 keV.

## II. EXPERIMENTAL CONDITIONS

The TESSA array, equipped with 16 Compton-suppressed Ge detectors, was positioned at the H1B external neutron beam at the HFBR, such that the beam passed through the center of the array. A bismuth filter was used to provide a thermal neutron beam with an intensity of  $7 \times 10^6 n_{\text{th}}/\text{cm}^2/\text{sec}$ . A collimator was selected to give a 1 cm diameter beam. A target of  $\sim 500$  mg  $\text{Er}_2\text{O}_3$  powder, enriched to 91.54% in  $^{167}\text{Er}$ , was placed in the center of the array, 20 cm from the Ge detectors. The data acquisition system stored the analog to digital converter (ADC) addresses, giving the energies deposited in the detectors, detector number tags, and the time to amplitude converter (TAC) addresses, giving the time intervals between coincident signals, for each event. The data were stored on 8 mm tape for later analysis. The ADC's had a range of 4096 channels, and the amplifier gains were set to correspond to  $\sim 1$  keV per channel, which gave a useful upper limit of  $\sim 3800$  keV. In all,  $1.5 \times 10^8$  two-detector coincidence events were obtained in the true and random TAC gates. Coincidence data were collected over a 4 day period. In comparison, the data for Ref. [6] required 2 months of beam time.

## III. DATA ANALYSIS

The data tapes were sorted to select all events that involved two detectors. From this set of data, two matrices were constructed, one corresponding to events in a true time window, the other to events in a random time window. A

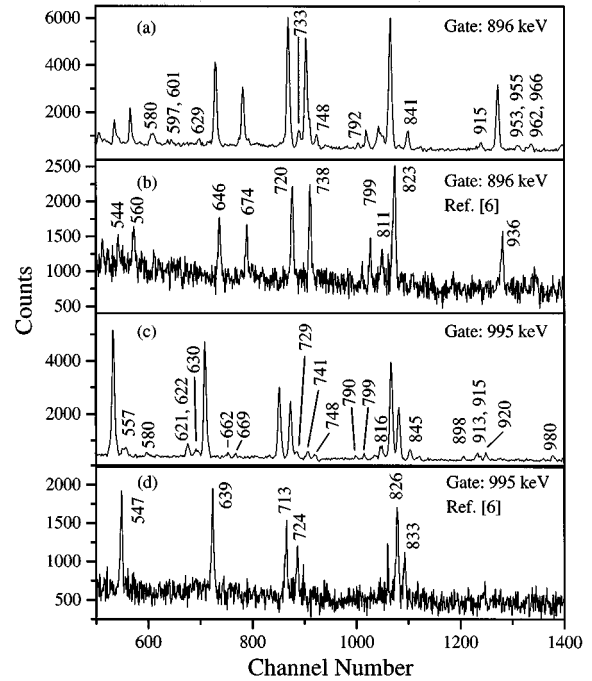


FIG. 2. A comparison of two gates from this experiment with that from Junglaus *et al.* [6] is shown. (a) and (c) are from this experiment, and (b) and (d) are from the corresponding data of Ref. [6]. The spectra from this experiment have been shifted so that the peaks approximately line up with those from Ref. [6]. Strong peaks are labeled in (b) and (d) (the Ref. [6] data), but not in (c) and (d) to avoid cluttering the figure.

gain shift was applied, as the matrices were built, to allow all two-detector events to be incorporated into the matrices. In this fashion, all the data (true and random) were included in two matrices. Thus, a random subtracted gate could easily be placed on a  $\gamma$  ray of interest, by projecting the desired channels out of the matrices.

Since the most recent  $^{168}\text{Er}$  level scheme [5] was based on the Ritz combination results of Davidson and Dixon [3], and since the work of Junglaus *et al.* [6] demonstrated that there are a number of assignments which are not supported by the coincidence data, the older level scheme [4] was used as the starting point to search for new levels. Gates were placed on strong transitions depopulating 64 excited states in order to locate  $\gamma$  rays that feed into known levels from higher, unknown levels. Each resulting spectrum was analyzed for expected  $\gamma$  transitions and for previously unobserved coincidences. Because of the large number of  $\gamma$  rays that deexcite levels in  $^{168}\text{Er}$  and the gain that was selected, it was sometimes difficult to obtain a desired gate that was free of  $\gamma$  rays in coincidence with nearby, interfering  $\gamma$  rays. For these reasons, gates could not be placed on 18 additional excited states. Figure 1 shows the projection of all two-fold  $\gamma$ - $\gamma$  events, which was used to select gate positions and which illustrates the above point. Another 13 excited states were not gated on because, although they are shown in the level scheme [4], there are no  $\gamma$  rays assigned to the depopulation of these levels. Nonetheless, it was possible to identify  $>250$  new coincidence relationships. Many of these are now observable due to the increased peak to the Compton ratio, made possible by the BGO shields, and to the large amount

of data that could be collected in a relatively short time, due to the increased number of detector pairs. The peak to Compton ratio in this experiment is  $\sim 4$  times larger than that in Ref. [6], and the effective number of detector pairs is 40 times larger. Figure 2 shows two gated spectra that are compared to those from the work of Jungclaus *et al.* [6].

Proposed levels from the present data were compared with those proposed by Ref. [3], as listed in [5], to identify common level assignments. When such levels were identified, the  $\gamma$  rays assigned to the level were compared to the present data to verify if their placement could be supported by coincidence. In some cases, it was necessary to set additional gates to test proposed placements.

#### IV. DISCUSSION

With the new coincidence data from the TESSA array, it was possible to place 26 additional  $\gamma$  rays between levels assigned in Ref. [5]. Table I lists those  $\gamma$  rays and the levels that they connect, along with the proposed spin and parity ( $J^\pi$ ) assignments in Ref. [5]. Throughout the discussion, wherever possible, the  $\gamma$ -ray energies used are those derived

from Ref. [2] which include bent crystal spectrometer measurements. These energies, and the levels deduced from them, provide higher precision than is possible with the current array measurements. In cases where the present data disagree with, or place additional restrictions on the  $J^\pi$  assignments, the new possible  $J^\pi$  are listed. Where multipolarity information is absent, it is assumed that only  $E1$ ,  $M1$ , and  $E2$  transitions need to be considered. In all further discussions of spin and parity assignments arising from this work, the above assumption will be used. The level assignments in Table I place restrictions on some  $J^\pi$  assignments, and conflict with others listed in Ref. [5]. Since each of these need to be presented in the context of other information, specifically that in Table III, the discussion of the modified assignments will be deferred until the discussion of Table III.

Table II lists 14 levels, newly established by coincidence, which were not identified by Davidson and Dixon [3], which can now be proposed on the condition that at least two  $\gamma$  rays depopulate the level and connect to known (i.e., listed in Ref. [5]) levels. Gates were set on  $\gamma$  rays that deexcited key levels. If more than one strong  $\gamma$  ray deexcited a level, those gates were summed together to improve the statistics of

TABLE I. Placement of  $\gamma$  rays between levels assigned in Ref. [5] that are supported by coincidences observed in this work. The  $J^\pi$  [this work] column gives possible  $J^\pi$  assignments when the new  $\gamma$ -ray placements lead to conflicts with or place additional restrictions on proposed assignments in Refs. [5,6].

$E_\gamma$ (keV)	Initial level (keV)	$J^\pi$ <sup>a</sup>	$J^\pi$ [this work]	Final level (keV)	$J^\pi$ [5]
154.120(6) <sup>b</sup>	2302.573(32)	$3^-$		2148.370(3)	$5^-$
361.834(5) <sup>b</sup>	2392.626(9)	$(4)^-$	$4^+$	2031.090(8)	$4^+$
511.504(15) <sup>b</sup>	2494.523(66)	$2^-, 3^-$ <sup>c</sup>	$3^-$	1983.042(3)	$5^-$
511.860(7) <sup>b</sup>	2425.759(40)	$2^+$		1913.900(6)	$3^-$
612.0(5) <sup>d</sup>	2348.569(14)	$4^-$		1736.688(2)	$4^+$
649.087(9)	2302.573(32)	$3^-$		1653.549(2)	$3^+$
761.112(47) <sup>b</sup>	2302.573(32)	$3^-$		1541.558(2)	$3^-$
877.072(17)	2188.417(70)	$5^+$		1311.463(2)	$6^-$
899.853(50)	2392.626(9)	$(4)^-$	$4^+$	1493.135(4)	$2^+$
1020.327(56)	2331.998(5)	$6^-$		1311.463(2)	$6^-$
1029.410(40)	2440.377(99)	$2^{+c}$	$5^+$	1411.098(2)	$4^+$
1176.424(49)	2440.377(99)	$2^{+c}$	$5^+$	1263.907(2)	$6^+$
1192.7(5) <sup>d</sup>	2186.736(6)	$(3)^+$		994.750(2)	$4^+$
1219.770(51)	2337.12(6)	$3^-$		1117.572(2)	$5^+$
1294.223(52) <sup>b</sup>	2558.46(27)	$3^-, 4^\pm, 5^-$ <sup>c</sup>	$5^-$	1263.907(2)	$6^+$
1304.1(3) <sup>d</sup>	2298.263(4)	$(5)^+$		994.750(2)	$4^+$
1317.424(56) <sup>b</sup>	2970.73(35)	$4^+, 5^+$		1653.549(2)	$3^+$
1322.6(2) <sup>d</sup>	2440.377(99)	$2^{+c}$	$5^+$	1117.572(2)	$5^+$
1338.4(2)	2455.922(54)	$3^+, 4^\pm, 5^+$ <sup>c</sup>		1117.572(2)	$5^+$
1342.436(70) <sup>b</sup>	2337.12(6)	$3^-$		994.750(2)	$4^+$
1353.78(10) <sup>b</sup>	2348.569(14)	$4^-$		994.750(2)	$4^+$
1417.053(25)	2411.712(62)	$4^-$		994.750(2)	$4^+$
1441.41(7) <sup>b</sup>	2558.46(27)	$3^-, 4^\pm, 5^-$ <sup>c</sup>	$5^-$	1117.572(2)	$5^+$
1489.8(2) <sup>d</sup>	2484.56(15)	$(3)^+$		994.750(2)	$4^+$
1617.79(12)	2513.674(51)	$(5)^-$	$4^-$	895.795(2)	$3^+$
2523.21(35)	2786.9(4)	$2^\pm, 3^\pm, 4^+$ <sup>c</sup>		264.089(2)	$4^-$

<sup>a</sup>All  $J^\pi$  assignments were taken from Ref. [5], unless indicated otherwise.

<sup>b</sup>This assignment disagrees with that in Ref. [5].

<sup>c</sup>This  $J^\pi$  assignment was taken from Ref. [6].

<sup>d</sup>This  $\gamma$  ray was not observed in previous studies.

TABLE II. Proposed new levels in  $^{168}\text{Er}$ , each of which was found to be depopulated by at least two  $\gamma$  rays. The  $\gamma$  intensity ( $I_\gamma$ ) is taken from Ref. [5] and is given in units of  $\gamma/10\,000$  neutron captures. The intensities for new  $\gamma$  rays are from this work and are listed in Table IV.

New level (keV)	$J^\pi$ [this work]	Deexciting $\gamma$ ray (keV) [5]	$I_\gamma$ [5]	Final level (keV)	$J^\pi$ [5]
2392.074(29)	$5^\pm, 6^+$	552.771(6)	2.6(4)	1839.348(2)	$5^+$
		655.392(29)	1.0(2)	1736.688(2)	$4^+$
		1080.4(2) <sup>a</sup>	2.4(6)	1311.463(2)	$6^-$
		1128.27(8)	5(1)	1263.907(2)	$6^+$
2529.072(32)	$4^+, 5^-$	614.996(24)	2.8(5)	1913.900(6)	$3^-$
		1265.0(2) <sup>a</sup>	1.7(9)	1263.907(2)	$6^+$
2540.302(60)	$3^+, 4^\pm, 5^+$	1422.58(8)	4(2)	1117.572(2)	$5^+$
2628.65(18)	$3^+, 4^\pm, 5^+$	1644.45(6)	13(3)	895.795(2)	$3^+$
		1511.1(3) <sup>a</sup>	3(2)	1117.572(2)	$5^+$
		1633.7(3)	3(1)	994.750(2)	$4^+$
2657.561(93) <sup>b</sup>	$2^-, 3^\pm, 4^\pm$	1732.76(16)	10(2)	895.795(2)	$3^+$
		1004.11(4)	4(1)	1653.549(2)	$3^+$
		1042.35(21)	2(1)	1615.343(2)	$4^-$
2673.04(10) <sup>b</sup>	$4^+, 5^\pm, 6^+$	1226.0(5) <sup>a</sup>	0.6(3)	1431.466(4)	$3^-$
		1409.15(4)	13(4)	1263.907(2)	$6^+$
2727.74(13) <sup>b</sup>	$3^+, 4^\pm, 5^\pm$	1677.2(5) <sup>a</sup>	2.1(7)	994.750(2)	$4^+$
		1112.41(5)	8(2)	1615.343(2)	$4^-$
		1611.4(5) <sup>a</sup>	4(2)	1117.572(2)	$5^+$
2738.475(69) <sup>b</sup>	$3^-, 4^\pm, 5^\pm, 6^-$	1732.76(16)	10(2)	994.750(2)	$4^+$
		1030.50(5)	5(1)	1707.995(2)	$5^-$
		1123.30(6)	6(1)	1615.343(2)	$4^-$
2740.16(19)	$4^+, 5^\pm, 6^+$	1476.0(3) <sup>a</sup>	0.6(3)	1263.907(2)	$6^+$
		1622.0(5) <sup>a</sup>	2(1)	1117.572(2)	$5^+$
		1745.58(18)	7(2)	994.750(2)	$4^+$
2768.816(21)	$3^-, 4^\pm, 5^\pm, 6^-$	1060.06(13)	2.4(9)	1707.995(2)	$5^-$
		1153.31(6)	2.4(7)	1615.343(2)	$4^-$
2849.8(4) <sup>b</sup>	$3^-, 4^+, 5^\pm,$ $6^\pm, 7^-$	1141.46(7)	3(1)	1707.995(2)	$5^-$
		1585.89(24)	5(2)	1263.907(2)	$6^+$
2852.149(18)	$3^+, 4^\pm, 5^\pm, 6^-$	792.11(6)	1.9(7)	2059.976(2)	$4^-$
		1734.4(5) <sup>a</sup>	<4(2)	1117.572(2)	$5^+$
2896.40(13) <sup>b</sup>	$2^-, 3^\pm, 4^\pm, 5^-$	1281.03(7)	10(3)	1615.343(2)	$4^-$
		1355.3(3) <sup>a</sup>	67(8)	1541.558(2)	$3^-$
2982.254(20)	$3^\pm, 4^\pm, 5^\pm$	1366.914(20)	23(6)	1615.343(2)	$4^-$
		1987.77(10)	5(2)	994.750(2)	$4^+$

<sup>a</sup>This  $\gamma$  ray was not observed in previous studies.

<sup>b</sup>Denotes levels that were listed in Ref. [5], but were not assigned any depopulating  $\gamma$  rays.

events that feed into the level. The energies of all the new levels are based on summing the coincident (feeding)  $\gamma$ -ray energy (as reported in Ref. [5]) with the level energy appropriate to the gate. In cases where the coincident  $\gamma$  ray was seen in several gates (representing directly cascading levels), the  $\gamma$  energy was summed to the highest coincident level energy. No attempt was made to use these new levels, or the newly proposed levels in Refs. [3,6], to find additional levels to fit other, unassigned  $\gamma$  rays, into the level scheme. Some of the levels in Table II were listed in Ref. [5], based on the observation of primary  $\gamma$  rays from neutron capture, but were not assigned any depopulating transitions. Such levels, which were confirmed in this work, are also referred to as new levels. There is insufficient information to allow definitive  $J^\pi$  assignments to be made for any new levels. Table II lists the ranges of  $J^\pi$  assignments that are allowed by the

data from this experiment. The new levels are also shown in Fig. 3 which shows the final (known) levels that each new level decays to.

Table III shows a comparison of the assignment of  $\gamma$  rays that depopulate new levels, proposed by Ref. [3] and adopted in Ref. [5], to the assignments that can be supported by coincidences from the present study. It also includes levels that were proposed in Ref. [6] in order to provide a vehicle for comparison to the present coincidence data. The spin assignments made in Refs. [5,6] are given in the table, below the level energy from those references. The level energy from this work is derived from the weighted average of the sums of the final level and deexciting  $\gamma$ -ray energies, using only those  $\gamma$  rays that are supported by the present experiment. The ranges of spin and parity assignments allowed by the present experiment are listed under the corresponding level



TABLE III. Levels listed in Refs. [3,6] that have been confirmed by coincidences observed in this experiment. For each level, all of the assigned  $\gamma$  rays (from Refs. [3,6] and the present work) are listed along with a note indicating the status of that placement in this work. The level energy is recalculated using only those  $\gamma$  rays that are supported by this work, as indicated by the notations ‘‘a’’ or ‘‘d.’’

$E_{\text{level}}$ (keV) $J^\pi$ [5,6]	Deexciting $\gamma$ ray (keV)	$I_\gamma$ (relative)	Mul [5]	Final level [5]	$J^\pi$	Note	$E_{\text{level}}$ (keV) $J^\pi$ [this work]
2188.377(8) $5^+$	226.98(3)	<0.50		1961.400(2)	$6^+$	a	2188.471(70) $4^-, 5^\pm, 6^+$
	348.94(3)	<1.6		1839.348(3)	$5^+$	b	
	367.904(9)	2.1(4)		1820.477(3)	$5^-$	c	
	451.68(3)	1.1(4)		1736.688(2)	$4^+$	b	
	534.793(15)	3.5(6)		1653.549(2)	$3^+$	b	
	877.072(17)	13(4)		1311.463(2)	$6^-$	d	
	995.306(25)	36(6)		1193.026(2)	$5^-$	e	
	1292.66(4)	50(14)	$E2$	895.795(2)	$3^+$	c	
	1639.73(10)	32(9)		548.745(2)	$6^+$	b	
	1924.36(13)	100(23)		264.089(2)	$4^+$	e	
2188.573(4) $2^+, 3^\pm, 4^+$	349.229(3)	9(3)	$M1$	1839.348(3)	$5^+$	c	2188.74(11) $2^+, 3^\pm, 4^+$
	1194.08(16)	42(17)		994.750(2)	$4^+$	e	
	2108.85(15)	100(27)		79.804(1)	$2^+$	e	
2193.20(4) $(2)^+$	1297.32(6)	39(12)		895.795(2)	$3^+$	e	2193.187(67) $1^+, 2^\pm, 3^+$
	1372.05(4)	100(25)	$M1$	821.169(2)	$2^+$	e	
2238.178(3) $4^+$	178.189(20)	0.25(5)		2059.976(2)	$4^-$	c	2238.180(71) $4^\pm, 5^\pm$
	333.086(4)	2.1(3)		1905.092(3)	$4^-$	a	
	345.247(7)	1.6(3)		1892.936(2)	$4^-$	e	
	389.804(4)	<0.78		1848.351(5)	$2^+$	c	
	398.829(3)	1.03(20)		1839.348(2)	$5^+$	e	
	501.506(10)	6.4(9)		1736.688(2)	$4^+$	e	
	1045.31(7)	4.9(17)		1193.026(2)	$5^-$	e	
	1144.112(11)	100(12)	$E1$	1094.040(2)	$4^-$	c	
2262.695(10) $(3)^-$	263.421(18)	1.3(3)		1999.224(3)	$3^-$	e	2262.693(35) $2^+, 3^\pm, 4^\pm$
	609.164(9)	9.6(13)		1653.549(2)	$3^+$	e	
	629.184(20)	17(4)		1633.461(3)	$3^-$	e	
	647.344(15)	15(3)	$E2$	1615.343(2)	$4^-$	a	
	1267.83(10)	43(13)		994.750(2)	$4^+$	e	
	1366.914(20)	100(26)		895.795(2)	$3^+$	e	
	1441.41(7)	<83	$E1$	821.169(2)	$2^+$	c	
2273.579(21) $(4^+)$	1009.675(21)	100(14)	$E2$	1263.907(2)	$6^+$	c	2273.663(91) $2^+, 3^\pm, 4^+$
	1276(4)		$E2$	994.750(2)	$4^+$	c	
	1376(6)			895.795(2)	$3^+$	b	
	1452.50(11)	33(15)		821.169(2)	$2^+$	e	
	2009.56(16)	47(12)		264.089(2)	$4^+$	e	
	2089.347(3)	0.27(10)		2089.347(3)	$4^-$	c	
2298.260(3) $(5)^+$	296.309(6)	1.3(3)		2002.471(5)	$(4)^+$	c	2298.263(4) $5^\pm, 6^+$
	458.910(3)	5.7(10)	$M1$	1839.338(2)	$5^+$	e	
	986.94(5)	15(3)		1311.463(2)	$6^-$	e	
	1105.260(10)	100(13)	$E1$	1193.026(2)	$5^-$	e	
	1304.1(3)	10(3)		994.750(2)	$4^+$	d,f	
	154.120(5)	1.7(6)		2148.370(3)	$5^-$	d	
2302.685(5) $3^-$	409.751(6)	4.1(9)		1839.348(2)	$5^+$	c	2302.573(32) $3^-$
	474.636(17)	4.9(9)		1828.065(2)	$3^-$	a	
	482.190(20)	4.1(8)		1820.477(3)	$5^-$	c	
	583.472(22)	13(3)		1719.179(3)	$4^-$	c	
	649.087(9)	16(5)		1653.549(2)	$3^+$	d	
	669.221(20)	41(7)		1633.461(3)	$3^-$	e	
	687.30(3)	68(12)		1615.343(2)	$4^-$	e	
	733.231(10)	34(8)	$M1$	1569.452(3)	$2^-$	e	
	761.112(47)	21(7)		1541.558(2)	$3^-$	d	

TABLE III. (Continued).

$E_{\text{level}}$ (keV) $J^\pi$ [5,6]	Deexciting $\gamma$ ray (keV)	$I_\gamma$ (relative)	Mul [5]	Final level [5]	$J^\pi$	Note	$E_{\text{level}}$ (keV) $J^\pi$ [this work]
	1406.93(7)	70(2)		895.795(2)	3 <sup>+</sup>	e	
	1481.71(13)	100(20)		821.169(2)	2 <sup>+</sup>	e	
2331.987(3)	131.566(2)	22(5)		2200.421(3)	5 <sup>-</sup>	a	2331.998(5)
6 <sup>-</sup>	381.181(14)	25(3)		1950.808(2)	7 <sup>-</sup>	a	4 <sup>-</sup> , 5 <sup>±</sup> , 6 <sup>±</sup> , 7 <sup>-</sup>
	382.346(9)	32(6)	M1	1949.638(3)	(6) <sup>-</sup>	a	
	511.504(15)	64(12)		1820.477(3)	5 <sup>-</sup>	c	
	511.860(7)	100(16)		1820.134(2)	6 <sup>-</sup>	c	
	624.005(5)	92(12)		1707.995(2)	5 <sup>-</sup>	e	
	1020.327(56)	244(50)		1311.463(2)	6 <sup>-</sup>	d	
2345.295(24)	322.910(6)	1.3(4)		2022.329(6)	3 <sup>-</sup>	c	2345.19(15)
3 <sup>-</sup>	1449.26(12)	50(26)		895.795(2)	3 <sup>+</sup>	e	1 <sup>-</sup> , 3 <sup>-</sup>
	1524.18(13)	100(29)	E1	821.169(2)	2 <sup>+</sup>	e	
	2081.15(35)	21(9)		264.089(2)	4 <sup>+</sup>	c	
2348.560(5)	259.209(5)	<3		2089.347(3)	4 <sup>-</sup>	c	2348.569(14)
4 <sup>-</sup>	612.0(5)	200(100)		1736.688(2)	4 <sup>+</sup>	d,f	4 <sup>±</sup> , 5 <sup>±</sup>
	629.397(20)	70(17)		1719.179(3)	4 <sup>-</sup>	e	
	640.567(20)	<27		1707.995(3)	5 <sup>-</sup>	e	
	695.04(4)	13(4)		1653.549(2)	3 <sup>+</sup>	b	
	1155.56(3)	79(23)	M1	1193.026(2)	5 <sup>-</sup>	b	
	1231.04(9)	57(3)		1117.572(2)	5 <sup>+</sup>	e	
	1353.78(10)	600(300)	E2	994.750(2)	4 <sup>+</sup>	d	
	1452.50(11)	100(43)		895.795(2)	3 <sup>+</sup>	c	
2382.582(9)	351.422(14)	1.8(6)		2031.090(8)	4 <sup>+</sup>	b	2382.590(49)
2 <sup>+</sup>	383.366(3)	44(12)	E1	1999.224(3)	3 <sup>-</sup>	e	2 <sup>+</sup> , 3 <sup>±</sup> , 4 <sup>+</sup>
	1486.78(8)	100(27)		895.795(2)	3 <sup>+</sup>	e	
	2303.22(20)	80(29)		79.804(1)	2 <sup>+</sup>	e	
	2382.22(24)	40(17)		0.0	0 <sup>+</sup>	a	
2392.626(9)	361.834(5)	7(3)	M1	2031.090(8)	4 <sup>+</sup>	d	2392.846(57)
(4) <sup>-</sup>	684.654(15)	<11.1		1707.995(2)	5 <sup>-</sup>	e	4 <sup>+</sup>
	759.157(10)	5.6(17)		1633.461(3)	3 <sup>-</sup>	c	
	899.853(50)	12(7)		1493.135(4)	2 <sup>+</sup>	d	
	1199.61(4)	43(11)	E2	1193.026(2)	5 <sup>-</sup>	e	
	1275.32(9)	100(39)		1117.572(2)	5 <sup>+</sup>	e	
	1298.40(9)	40(13)		1094.040(2)	4 <sup>-</sup>	c	
	1398.05(6)	67(22)		994.750(2)	4 <sup>+</sup>	e	
	1496.76(13)	28(11)		895.795(2)	3 <sup>+</sup>	c	
2398.553(65)	1281.034(68)	56(21)		1117.572(2)	5 <sup>+</sup>	e	2398.577(54)
4 <sup>+</sup> , 5 <sup>+</sup>	1502.73(9)	100(22)		895.795(2)	3 <sup>+</sup>	e	4 <sup>+</sup> , 5 <sup>+</sup>
2402.38(7)	1407.67(9)	18(5)		994.750(2)	4 <sup>+</sup>	e	2401.12(26)
	1506.49(12)	47(12)	E1	895.795(2)	3 <sup>+</sup>	b	2 <sup>+</sup> , 3 <sup>±</sup> , 4 <sup>+</sup>
	1580.72(8)	100(11)	E1	821.169(2)	2 <sup>+</sup>	e	
	2322.51(8)	26(8)		79.804(1)	2 <sup>+</sup>	c	
	2401.92(24)	21(6)		0.0	0 <sup>+</sup>	a	
2411.640(22)	1100.11(15)	8(11)		1311.463(2)	6 <sup>-</sup>	e	2411.712(62)
4 <sup>-</sup>	1218.68(7)	<33		1193.026(2)	5 <sup>-</sup>	e	4 <sup>-</sup> , 5 <sup>+</sup> , 6 <sup>+</sup>
	1294.053(25)	100(29)	E1	1117.572(2)	5 <sup>+</sup>	e	
	1317.56(10)	24(7)		1094.040(2)	4 <sup>-</sup>	c	
	1417.053(25)	71(28)	M1	994.750(2)	4 <sup>+</sup>	d	
	1515.99(6)	<240	E1	895.795(2)	3 <sup>+</sup>	c	
2425.42(6)	511.860(7)	17(4)		1913.900(6)	3 <sup>-</sup>	d	2425.759(40)
2 <sup>+</sup>	1208.30(9)	<29		1217.160(14)	0 <sup>+</sup>	a	1 <sup>-</sup> , 2 <sup>±</sup> , 3 <sup>±</sup> , 4 <sup>+</sup>
	1529.67(17)	20(7)		895.795(2)	3 <sup>+</sup>	c	
	1604.09(18)	33(13)		821.169(2)	2 <sup>+</sup>	e	
	2345.58(17)	100(20)		79.804(1)	2 <sup>+</sup>	c	

TABLE III. (Continued).

$E_{\text{level}}$ (keV) $J^\pi$ [5,6]	Deexciting $\gamma$ ray (keV)	$I_\gamma$ (relative)	Mul [5]	Final level [5]	$J^\pi$	Note	$E_{\text{level}}$ (keV) $J^\pi$ [this work]
	2425.35(20)	100(20)		0.0	$0^+$	a	
2440.069(9)	445.234(20)	0.7(2)		1994.819(4)	$(3)^+$	a	2440.377(99)
$2^+$	526.079(7)	1.0(3)		1913.900(6)	$3^-$	c	$5^+$
	1029.410(40)	3.2(8)		1411.098(2)	$4^+$	d	
	1176.424(49)	8(2)	$M1$	1263.907(2)	$6^+$	d	
	1223.00(7)	4(2)		1217.160(14)	$0^+$	c	
	1322.6(2)	100(9)		1117.572(2)	$5^+$	d,f	
	1445.26(8)	3(2)		994.750(2)	$4^+$	e	
2455.721(14)	267.359(8)	1.0(4)		2188.377(8)	$5^+$	a	2455.922(54)
$3^+, 4^\pm, 5^+$	1338.4(2)	23(10)		1117.572(2)	$5^+$	d	$3^+, 4^\pm, 5^+$
	1461.13(8)	36(11)		994.750(2)	$4^+$	e	
	1560.16(8)	100(18)		895.795(2)	$3^+$	e	
	2191.48(20)	50(16)		264.089(2)	$4^+$	c	
2478.09(11)	1484.46(8)	94(30)	$E1$	994.750(2)	$4^+$	e	2478.68(32)
$(3^+)$	1582.95(20)	50(17)		895.795(2)	$3^+$	e	$3^-$
	1656.84(9)	<44		821.169(2)	$2^+$	e,g	
	2214.47(20)	72(17)		264.089(2)	$4^+$	e	
	2398.25(15)	100(222)		79.804(1)	$2^+$	c	
2494.021(75)	511.504(15)	8(2)		1983.042(3)	$5^-$	d	2494.523(66)
$2^-, 3^-$	1672.84(9)	42(12)	$E1$	821.169(2)	$2^+$	e	$3^-$
	2229.27(20)	26(11)		264.089(2)	$4^+$	e	
	2414.33(19)	42(12)		79.804(1)	$2^+$	e	
2513.70(6)	1396.12(6)	100(36)		1117.572(2)	$5^+$	e	2513.674(51)
$(5^-)$	1518.95(16)	82(27)	$E1$	994.750(2)	$4^+$	e	$4^-$
	1617.79(12)	100(41)	$E1$	895.795(2)	$3^+$	d	
2558.637(47)	235.652(18)	0.4(11)		2323.20(9)	$3^-$	a	2558.46(27)
$3^-, 4^\pm, 5^-$	984.419(77)	4(1)		1574.117(3)	$5^-$	b	$5^-$
	1199.610(37)	15(5)	$E2$	1358.898(5)	$1^-$	a	
	1294.223(52)	100(19)	$E1$	1263.907(2)	$6^+$	d	
	1441.41(7)	36(8)	$E1$	1117.572(2)	$5^+$	d	
	1563.85(9)	28(8)		994.750(2)	$4^+$	e	
2660.447(7)	471.874(6)	13(4)		2188.377(8)	$5^+$	a	2660.492(76)
$4^+, 5^+$	512.133(24)	28(9)		2148.370(3)	$5^-$	c	$3^+, 4^\pm, 5^+$
	1542.94(25)	75(31)		1117.572(2)	$5^+$	e	
	1665.74(8)	100(25)	$M1$	994.750(2)	$4^+$	e	
2786.390(29)	308.309(5)	9(9)		2478.09(11)	$(3^+)$	c	2786.46(12)
$2^\pm, 3^\pm, 4^+$	384.510(9)	7(3)		2402.38(7)	$(4)^-$	e	$2^-, 3^\pm, 4^+$
	1890.93(35)	57(33)		895.795(2)	$3^+$	e	
	1965.19(15)	100(29)		821.169(2)	$2^+$	e	
	2523.21(35)			264.089(2)	$4^-$	d	
2969.694(93)	1317.424(56)	31(15)		1653.549(2)	$(3)^+$	d	2970.73(35)
$4^+, 5^+$	1875.69(12)	56(19)	$E1$	1094.040(2)	$4^-$	e	$3^+, 4^+, 5^+$
	1975.08(30)	56(19)		994.750(2)	$4^-$	e	
	2420.71(24)	100(25)		548.745(2)	$6^+$	c	

<sup>a</sup>No gate could be set to test this placement.

<sup>b</sup>This  $\gamma$  ray was obscured by another in the coincidence spectrum, but the placement here is possible.

<sup>c</sup>This  $\gamma$  ray was not observed in the coincidence gate.

<sup>d</sup>Additional  $\gamma$  ray observed in this work to deexcite this level.

<sup>e</sup>The proposed placement of this  $\gamma$  ray is confirmed.

<sup>f</sup>This  $\gamma$  ray was not observed in previous studies.

<sup>g</sup>Multiple placements are assigned to this  $\gamma$  ray.

state, the key connection that limits the  $J^\pi$  assignment to  $2^+$ , cannot be confirmed.

2392.846 keV. This level is listed as a  $4^-$  state in Ref. [3], but the new information presented here indicates that it is

more likely a  $4^+$  state. The observation of the 361.8 keV  $M1$  transition (see Tables I and III) to the  $4^+$  2031 keV level requires a positive parity. The newly placed 899.9 keV transition to the  $2^+$  1493 keV level suggests a spin no higher

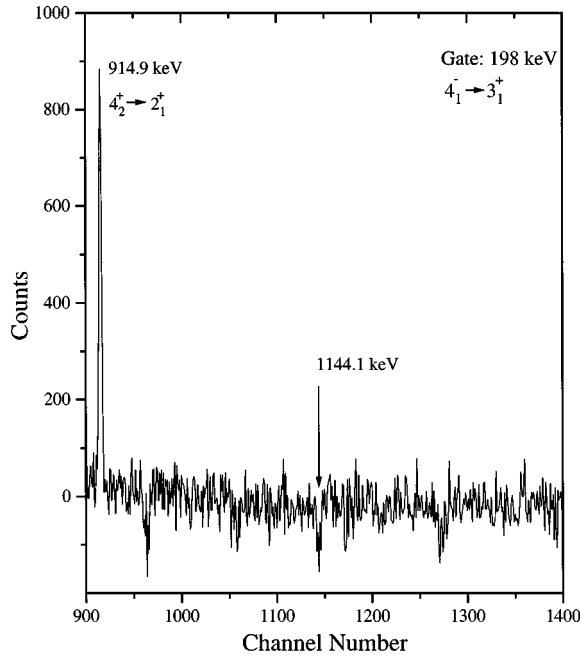


FIG. 4. A portion of the spectrum from gating on the 198.24 keV  $\gamma$  ray, which deexcites the 1094 keV level, is shown. According to Ref. [3], the 1144.1 keV  $\gamma$  ray is the strongest  $\gamma$  ray that deexcites the 2238 keV level, feeding the 1094 keV level, and therefore must be prominent in this gate. However, as can be seen in the figure, there is no evidence of any peak in the 1144 keV region of this coincidence spectrum.

than 4 is allowed. This information, combined with the transitions to states with spin 5 (see Table III), limits the level to  $J^\pi$  of  $4^+$ .

**2398.577 keV.** This level corresponds to the 2398.553 keV level in [6] and the 2398.1 keV level in [5]. All of the  $\gamma$  rays that were proposed to deexcite this level in Ref. [6] are observed here, except for the 5373 keV  $\gamma$  ray, which is above the range of the present experiment.

**2401.12 keV.** This level was proposed in Ref. [6]. In the present experiment, the 2322.5 keV  $\gamma$  ray is not observed in coincidence in the 80 keV gate. The 2402 keV transition to the ground state is not seen here, since no  $\gamma$  rays that feed the 2402 keV level (other than primary neutron capture  $\gamma$  rays) have been observed in this or other experiments. The primary  $\gamma$  ray cannot be gated on since it is above the energy range of the current experiment.

**2411.712 keV.** This level probably corresponds to the one listed in Ref. [5] at 2411.640 keV and assigned a  $J^\pi$  of  $4^-$  by Ref. [3]. The present data do not support the placement of  $\gamma$  transitions to the 896 and 1094 keV states. Thus, on the basis of the information in Table III, a unique  $J^\pi$  assignment cannot be made.

**2425.759 keV.** The Ritz combination employed by Ref. [3] indicates that this level is a  $2^+$  state, and has been proposed as the bandhead of a  $K^\pi=2^+$  band. The coincidence data obtained here support only one of the  $\gamma$  rays (the transition to the 821 keV level) placed by [3]. Only one additional  $\gamma$  ray, at 511.9 keV, is also placed at this level. Thus, a unique assignment of  $2^+$  cannot be supported.

**2440.377 keV.** A level at 2439.7 keV is listed in Ref. [5], without deexcitation information, and a  $2^+$  level at 2440.069

keV was proposed by Jungclaus *et al.* [6]. However, the placements of  $\gamma$  transitions to the 1217 keV  $0^+$  state and the  $3^-$  1914 keV state are not supported in the TESSA experiment. Thus, the unique assignment of  $2^+$  cannot be supported. A new  $\gamma$  ray at 1322.6 keV (see Table IV) is observed to depopulate this level to the 1118 keV  $5^+$  state. This combined with newly observed transitions to  $4^+$  and  $6^+$  states (see Table III) requires a  $J^\pi$  assignment of  $5^+$  for this level.

**2455.922 keV.** This level was observed in [6] and listed, without deexcitation information, in Ref. [5]. The present coincidences do not support the placement of the 2192 and 267 keV  $\gamma$  rays as depopulating this level, as reported in [6]. All of the transitions observed to deexcite this level, feed levels in the  $\gamma$  band.

**2478.68 keV.** The assignments leading to this level in Ref. [6] are all supported by the present coincidence measurements. This level corresponds to the level at 2479.21 keV listed in Ref. [5]. The Ritz combinations used in Ref. [3] place the 2398.3 keV  $\gamma$  ray as the strongest transition depopulating this level. However, that assignment is not supported by the present coincidence experiment. Since the 1484.5 keV transition is an  $E1$  to the 995 keV  $4^+$  state, the 2479 keV level is most likely a  $3^-$  state.

**2494.523 keV.** The present coincidence measurements support the level at 2495 keV observed by [6] and are consistent with the possible spin assignments given therein. The observation of the 511.5 keV transition to the  $5^-$  state at 1983 suggests that the level at 2495 keV is a  $3^-$  state.

**2513.674 keV.** A level is listed in [5] at 2513.7 keV. The coincidence data here identifies another  $\gamma$  ray, at 1617.8 keV, which deexcites this level. Since this  $\gamma$  transition is an  $E1$  transition to the 896 keV  $3^+$  state, the 2513.7 keV level must be a  $4^-$  state, rather than  $(5)^-$  as suggested in Ref. [5].

**2558.637 keV.** This level has the same energy as a level proposed in Ref. [6]. However, only one of the four  $\gamma$  rays (see Table III) that should have been observed in the present experiment could be assigned to the decay of this level. Reference [5] also lists a level at 2558.8 keV. The new coincidence information in Table III places two  $E1$  transitions as deexciting the 2559 keV level to  $5^+$  and  $6^+$  states. This information leads to a unique assignment of  $J^\pi=5^-$  for this level.

**2660.447 keV.** This level was proposed by Jungclaus *et al.* in Ref. [6]. Here only two of the deexciting  $\gamma$  rays are observed.

**2786.46 keV.** This new level was reported in Ref. [6]. All of the  $\gamma$  rays that were reported to deexcite this level are observed here, except the 308 keV  $\gamma$  ray. This  $\gamma$  ray was not observed in the gate on the  $\gamma$  rays that deexcite the 2478 keV level. A level at 2786.9 keV was also reported in [5] that probably corresponds to this level.

**2970.73 keV.** This new level was reported in Ref. [6]. All of the  $\gamma$  rays that were reported to deexcite this level are observed here, except the 2421 keV  $\gamma$  ray. This  $\gamma$  ray was not observed in the gate on  $\gamma$  rays that deexcite the 549 keV level. As a consequence, the possibility that the 2971 keV level may be a  $3^+$  state cannot be ruled out.

In addition to the levels from Ref. [6] that were discussed above, two other levels proposed in that work are not supported by the data here. The levels at 2517.4 and 2551.6 keV

TABLE IV. New  $\gamma$  rays observed from the decay of  $^{168}\text{Er}$  using the TESSA spectrometer. Each  $\gamma$  ray is listed with the  $\gamma$  ray that it is observed to be in coincidence with. When a level assignment has been made, the assignment is also listed.

New $\gamma$ (keV)	Intensity ( $\gamma/10\,000n$ )	Coincident $\gamma^a$ (keV)	Assignment <sup>b</sup>
612.0(5)	7(5)	543.667 840.890	2348.4 $\rightarrow$ 1736.7
847.7(2)	2.1(5)	619.990	
916.0(5)		1786.09	
1047.2(2)		1323.913	
1080.4(2)	2.4(6)	217.422 840.890	2392.8 $\rightarrow$ 1311.5
1124.8(2)	2.5(5)	217.422	
1126.8(3)	0.1(1)	1892.932	
1192.7(5)	4(1)	730.660 914.944	2186.7 $\rightarrow$ 994.8
1226.0(5)	0.6(3)	1167.396 1351.54	2657.6 $\rightarrow$ 1431.5
1240.9(3)	1.1(5)	619.990	
1250.9(2)	2.1(3)	673.666 748.281	
1256.3(5)	0.8(2)	422.318	
1256.8(3)	18(4)	559.510	
1265.0(2)	1.7(9)	715.163 999.827	
1304.1(3)	2.9(9)	730.660 914.944	2298.3 $\rightarrow$ 994.8
1322.6(2)	8(4)	568.821 853.473	2440.4 $\rightarrow$ 1117.6
1330.7(3)	2.1(5)	217.422	
1355.3(3)	67(8)	447.517 720.382	2896.4 $\rightarrow$ 1541.6
1356.4(3)	6(3)	568.821 853.473	
1364.2(4)	3.4(4)	422.318	
1476.0(3)	0.6(3)	715.163 999.827	2740.2 $\rightarrow$ 1263.9
1489.2(2)	4(2)	730.660 914.944	2484.6 $\rightarrow$ 994.8
1511.1(3)	3(2)	568.821 853.473	2628.6 $\rightarrow$ 1117.6
1512.0(5)	0.7(4)	715.163 999.827	
1606.0(5)	4(1)	730.660 914.944	
1611.4(5)	4(2)	568.821 853.473	2727.7 $\rightarrow$ 1117.6
1622.0(5)	2(1)	568.821 853.473	2740.2 $\rightarrow$ 1117.6
1677.2(5)	2.1(7)	730.660 914.944	2673.0 $\rightarrow$ 994.8
1734.4(5)	<4(2) <sup>c</sup>	568.821 853.473	2852.1 $\rightarrow$ 1117.6
1751.6(5)	17(4)	741.356	
2279.8(5)	6(3)	741.356	
2498.5(5)	0.7(3)	1146.998 1331.324	
2577.6(5)	<12(3) <sup>c</sup>	284.655	
2606.2(5)	10(3)	741.356	

<sup>a</sup> $\gamma$ -ray energies are the accepted values from Nuclear Data Sheets (Ref. [5]).

<sup>b</sup>Level energies are nominal values given for identification purposes only.

<sup>c</sup>These lines appear to be multiplets. All of the intensity of the multiplet has been attributed to the listed line.

could not be confirmed by the present set of coincidence data. Key gates for each level had multiplets near the expected energies, but due to interference, a definitive identification could not be made. For the 2517.4 keV level, the weak 409 keV  $\gamma$  was not observed, even though no interference were present. Similarly, for the 2551.6 keV level, the weak 443 and 313 keV  $\gamma$  rays were not observed.

Table IV lists the new  $\gamma$  rays that were observed in the coincidence data taken in this experiment. The transitions that each new  $\gamma$  ray is observed to be in coincidence with is listed, along with the proposed, if any, placement of the new  $\gamma$  ray.

## V. CONCLUSIONS

The data on  $\gamma$  rays in  $^{168}\text{Er}$  taken with the TESSA array have led to a large number of new coincidence relationships which were used to allocate depopulating  $\gamma$  rays to several previously proposed levels. In addition a large number of new levels were revealed (Tables II and III) and many previously unobserved  $\gamma$  rays (Table IV) were observed. These data represent a marked improvement over the data of Jungclaus *et al.* of Ref. [6], as evidenced by the comparison in Fig. 2. The use of Compton-suppressed Ge detectors not only improved the peak to Compton ratio in any given spectrum, but assured that a greater fraction of the overall events collected would be nonrandom photopeak events. This gave a higher sensitivity to weak transitions, which would be missed in an experiment without the benefit of a Compton-suppressed array, such as TESSA. The experiment of Ref. [6] was able to detect  $\gamma$  rays with  $I_\gamma \geq 3/10\,000$  neutron captures, whereas the present experiment (see Table IV) was

sensitive to  $\gamma$  rays with  $I_\gamma \geq 0.1/10\,000$  neutron captures.

The comparison of the TESSA data with previous results (Table III) illustrates, again, the point that was made in Ref. [6]: Making level assignments solely on the basis of Ritz combinations is very risky, especially in cases, such as  $^{168}\text{Er}$ , where there are a large number of  $\gamma$  rays. Many such assignments will be correct; many will be incorrect. It is impossible to know which ones are correct and which are incorrect.

The purpose of the experiment was to test the usefulness of large arrays in low-spin studies of compound nuclear decay, via the  $(n, \gamma)$  reaction. To this end, an already well-studied nucleus  $^{168}\text{Er}$  with a large neutron capture cross section ( $\sim 600$  b) was chosen. The results are very encouraging and illustrate that large arrays can be very productive in neutron capture  $\gamma$ -ray spectroscopy, and should stimulate further studies of this type with such arrays. Possible areas of physics interest are the study of multiphonon states in spherical or deformed nuclei, which are a topic of high current interest and debate, the onset of chaos at excitation energies above the pairing gap, the study and testing of models of statistical decay of the capture state, and, eventually, the extension of nuclear structure interpretations into the region above the pairing gap.

## ACKNOWLEDGMENTS

This work was supported under Contract No. DE-AC02-76CH00016, Grant No. DE-FG02-91ER40609, and Contract No. W-31-109-ENG-38 with the U.S. Department of Energy, and by SERC Grant No. GR/J 95775 in the UK.

- 
- [1] J. F. Sharpey-Schafer and J. Simpson, *Prog. Part. Nucl. Phys.* **21**, 293 (1988); P. J. Nolan, D. W. Gifford, and P. J. Twin, *Nucl. Instrum. Methods Phys. Res. A* **236**, 95 (1985).
- [2] W. F. Davidson, D. D. Warner, R. F. Casten, K. Schreckenbach, H. G. Börner, J. Simić, M. Stojanović, M. Bogdanović, S. Koicki, W. Gelletly, G. B. Orr, and M. L. Stelts, *J. Phys. G* **7**, 455 (1981).
- [3] W. F. Davidson and W. R. Dixon, *J. Phys. G* **17**, 1683 (1991); National Research Council of Canada Report No. PIRS 0288, 1991.
- [4] V. S. Shirley, *Nucl. Data Sheets* **53**, 223 (1988).
- [5] V. S. Shirley, *Nucl. Data Sheets* **71**, 261 (1994).
- [6] A. Jungclaus, R. F. Casten, R. L. Gill, and H. G. Börner, *Phys. Rev. C* **49**, 88 (1994).